

DOI: 10.1002/cssc.201402605

Integrated, Cascading Enzyme-/Chemocatalytic Cellulose Conversion using Catalysts based on Mesoporous Silica Nanoparticles

Yi-Chun Lee, Saikat Dutta, and Kevin C.-W. Wu*^[a]

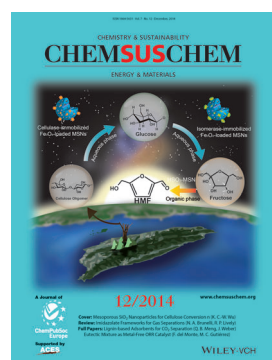
This article reports a novel approach to deconstructing cellulose into 5-hydroxymethylfurfural (HMF) with a high yield (46.1%) by integrating a sequential enzyme cascade technique in an aqueous system with solid acid catalysis in an organic-solvent system. We executed the rational design and synthesis of mesoporous silica nanoparticles (MSNs) with various pore sizes and surface functionalities, which proved to be useful for the immobilization of various enzymes (i.e., cellulase and isomerase) and nanoparticles (i.e., magnetic Fe₃O₄) and for functionalization of various acid groups (i.e., H₂PO₃, COOH, and SO₃H). We separately applied the synthesized biocatalysts (i.e., cellulase-Fe₃O₄@MSN and isomerase-Fe₃O₄@MSN) and chemical catalysts (i.e., HSO₃-MSN) in a sequential cellulose-to-glucose, glucose-to-fructose, and fructose-to-HMF conversion, respectively, across both aqueous- and organic-solvent systems after the optimization of reaction conditions (e.g., reaction temperature, water ratio, catalyst amount). The integrated enzymatic and chemocatalytic concept in this study could be an effective and economically friendly process for various catalytic applications.

plentiful renewable carbon. Enzyme-based biocatalysis is considered an alternative to the use of chemicals because enzyme-based biocatalysis provides higher product selectivity and can be triggered under milder reaction conditions.^[3] The consolidation of cascading enzymatic reactions in a single vessel has numerous benefits, such as decreased unit operations, decreased reactor volume, increased volumetric and space-time yields, and shortened cycle times. The major advantage of the cascading strategy is that the coupling of steps forces even unfavorable equilibria towards the formation of desired products.^[4] However, the major problems of cascading enzymatic reactions involve the stability and recyclability of the enzymes, particularly because the different enzymes are used under different reaction conditions. Therefore, researchers have preferred a method involving the preparation of magnetic and porous solid particles that can prevent enzymes from denaturing and allow easy recyclability.^[4]

We and other researchers have used mesoporous silica materials with large surface areas, adjustable pore sizes, and improved thermal stability as fillers,^[5] and diverse surface functionalities to immobilize enzymes.^[6] The encapsulated enzymes maintain their efficacy and show increased stability and recyclability. In particular, for cellulosic biomass conversion, we demonstrated that cellulase and glucose isomerase can be separately immobilized into iron oxide-encapsulated mesoporous silica nanoparticles (i.e., cellulase-Fe₃O₄@MSN and isomerase-Fe₃O₄@MSN) for cellulose-to-glucose and glucose-to-fructose conversion sequences, respectively.^[6d] The main advantage of such cascading enzymatic reactions is that the enzyme-immobilized Fe₃O₄@MSN material can be separated easily after each reaction, by using a magnet. In this manner, successful cascading of enzymatic reactions with a maximum fructose yield of 51% can be achieved under optimized reaction conditions, including buffer composition, reaction temperature time, and pH values. From a biofuel production perspective, scientists have considered further conversion of fructose to 5-hydroxymethylfurfural (HMF), a platform chemical, to be scientifically valuable but technologically challenging.^[7] Therefore, we attempted to solve this problem by integrating the enzyme cascade sequence in water systems with a chemical dehydration process for fructose-to-HMF conversion in an organic solvent system containing a series of functionalized MSN-based catalysts (Scheme 1).

Herein, we set out to achieve an effective cellulose-to-glucose-to-fructose-to-HMF conversion sequence by integrating a water (i.e., enzyme) system with an organic solvent (i.e., chemical) system. For water systems, we prepared enzyme-im-

Since researchers discovered the value of biomass as feedstock for the production of fuels, building-block chemicals, and advanced materials, a considerable amount of research has been conducted on the transformation of lignocellulosic biomass into commodity chemicals and liquid fuels, using numerous techniques, to reduce the dependence of the economy on petrochemicals.^[1] The physico-chemical recalcitrance of cellulose limits its rapid and cost-effective degradation.^[2]

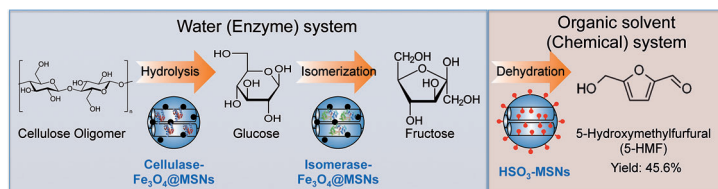


COVER

From the perspective of plant cell wall degradation, cellulytic and hemicellulytic enzymes that can deconstruct cellulose into fermentable sugars can facilitate the utilization of

[a] Y.-C. Lee, Dr. S. Dutta, Prof. Dr. K. C.-W. Wu
Department of Chemical Engineering
National Taiwan University
No. 1, Sec. 4, Roosevelt Road, Taipei 10617 (Taiwan)
E-mail: kevinwu@ntu.edu.tw

Supporting Information for this article is available on the WWW under <http://dx.doi.org/10.1002/cssc.201402605>.



Scheme 1. An integrated enzyme cascade-chemocatalytic conversion of cellulose oligomers into HMF in aqueous (enzyme) and organic (chemical) media with enzyme and acid functionalized mesoporous silica nanoparticles, respectively.

mobilized Fe_3O_4 @MSN materials to use as biocatalysts, and for chemical systems, we synthesized sulfonic-acid-functionalized MSN materials for use as catalysts. Only fructose-to-HMF conversions were run in organic solvent, because enzymatic conversions cannot be performed in such media. Therefore, in addition to the preparation of various MSN-based catalysts, optimization of reaction conditions such as the volume ratio of organic to aqueous phase and reaction temperature were critical for maximizing the final yield of HMF.

We modified a synthesis process of Fe_3O_4 nanoparticles and MSNs presented in a previous report,^[7d] and present details of the synthesis and functionalization processes using enzymes and acids in the Experimental Section. We also characterized the enzymes (cellulose, isomerase)-immobilized, Fe_3O_4 -loaded MSN and sulfonic-acid-functionalized MSN (HSO_3 -MSN) by using scanning electron microscopy (SEM), N_2 sorption isotherms, solid-state NMR, and UV-Vis spectroscopy. Table 1 summarizes the properties of the prepared MSN catalysts, including particle size, surface area and pore size, acidity, and acid amount.

We first synthesized magnetic Fe_3O_4 nanoparticles with particle sizes of approximately 20 nm and characterized these nanoparticles by transmission electron microscopy (TEM), powder X-ray diffraction (XRD), and superconducting quantum interference device (SQUID) measurements (Supporting Information, Figures S1–S3). We then added the synthesized Fe_3O_4 nanoparticles to the precursor used for MSN synthesis (Supporting Information, Figure S4). Subsequently, we used the synthesized Fe_3O_4 -loaded MSN (Fe_3O_4 @MSN) samples as hosts for the immobilization of enzymes. We maintained the particle sizes of the Fe_3O_4 @MSN between 500 and 600 nm and the pore size of the Fe_3O_4 @MSN at approximately 20 nm to efficiently immobilize cellulase (hydrodynamic diameter ca. 8 nm) and glucose isomerase (hydrodynamic diameter ca. 3 nm). We determined the amount of the immobilized enzyme by using UV-Vis spectroscopy, measuring absorbance at 280 nm. For

50 mg of Fe_3O_4 @MSN, the maximum amount of immobilized enzyme was 7.3 mg (36.5 units) for cellulase and 0.65 mg (19.1 units) for isomerase.

To prepare sulfonic acid-functionalized MSNs, we first synthesized MSNs with a small particle size (approximately 276 nm) and pore size (4.7 nm), and grafted the thiol-containing organosilane onto the MSNs. The thiol groups were then converted to sulfonic-acid groups through oxidation in the presence of H_2O_2 . We determined the acid strength (0.8–2.0) and amount ($1.29 \text{ mmol}(\text{H}^+) \text{g}^{-1}$) of the final HSO_3 @MSN material by using based an indicator (phenol red) and titration, respectively.

The enzyme-chemocatalytic cascading of the cellulose-to-HMF conversion involves three steps: (1) cellulose-to-glucose conversion (catalyst: cellulase- Fe_3O_4 @MSN), (2) glucose-to-fructose conversion (catalyst: isomerase- Fe_3O_4 @MSN), and (3) fructose-to-HMF conversion (catalyst: HSO_3 -MSN). We previously optimized the reaction conditions for the sequential reaction of the first two steps, and achieved a maximum yield of fructose (51%) under the following conditions: 50 °C, 24 h, and a phosphate buffer with pH 4.8 for cellulose-to-glucose conversion; and 70 °C, 24 h, and a phosphate buffer with pH 7.5 for glucose-to-fructose conversion.^[7d] The most difficult task is to continue the sequence from the first two steps in water-based systems to the third step in an organic solvent (i.e., DMSO)-based system. To solve this problem, we optimized three parameters: (1) reaction temperature and time, (2) the volume ratio of DMSO to water, and (3) the amount of HSO_3 -MSN catalyst.

Figure 1(a) indicates that temperature notably influences the yield of HMF. As the reaction temperature increased, the HMF yield also increased both with and without the HSO_3 -MSN catalyst. The fructose-to-HMF conversion is a dehydration reaction, therefore a higher reaction temperature is preferred, and numerous groups have used the same organic solvent (i.e., DMSO) at high temperatures to produce HMF.^[8] Apparently, the effect of the catalyst disappears at a high temperature (120 °C), possibly due to the electrophilic nature of DMSO at higher temperature. This facilitates formation of the α -furanose anomeric form of D-fructose at the expense of the β -pyranose form via the formation of a dihydrofuran-carbaldehyde intermediate, as reported based on direct spectroscopic evidence.^[8d]

An exception occurred at a temperature of 120 °C in the presence of the catalyst, which implies that such a high temperature produces intractable side products that decrease the HMF yield. At room temperature, an HMF yield of approximately 37% was achieved in the presence of the HSO_3 -MSN catalyst, in contrast to the 0% HMF yield without catalyst. This result clearly demonstrates the efficacy of our HSO_3 -MSN catalyst. However, based on the results of our study, we determined that 60 °C was the most economical and

Table 1. Characterization of enzyme- and acid-functionalized MSN-based catalysts.

Catalyst	Particle size ^[a] [nm]	Specific surface area ^[b] [$\text{m}^2 \text{g}^{-1}$]	Pore size ^[c] [nm]	Amount of enzyme ^[b] [mg]	Acidity ^[f] [pK_a]	Amount of acid ^[g] [$\text{mmol}(\text{H}^+) \text{g}^{-1}$]
cellulase- Fe_3O_4 @MSN	587.8	272.6	20.2	7.3	–	–
isomerase- Fe_3O_4 @MSN	645.1	283.1	20.4	0.65	–	–
HSO_3 -MSN	276.2	285.8	4.7	–	0.8–2.0	1.290

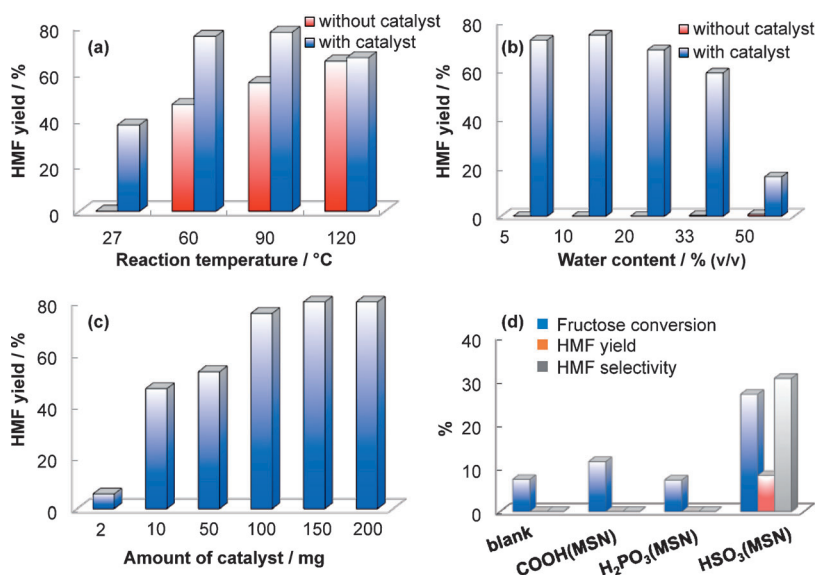


Figure 1. (a) Reaction temperature in fructose conversion to HMF in integrated method using HSO₃-MSN in DMSO media. (b) Effect of water/DMSO (v/v) on the HMF yield (%) with and without the HSO₃-MSN catalyst. (c) Influence of the loading amount of catalyst on the yield of HMF. (d) Effect of the different acid functionalities (COOH, H₂PO₃, HSO₃) of MSN catalysts on the fructose conversion and HMF yield.

efficient temperature for producing HMF (Supporting Information, Table S1).

Because we intended to integrate a water system with an organic solvent system, the amount of water in the final organic/aqueous biphasic system was critical for the final HMF yield. Figure 1(b) demonstrates that at a reaction temperature of 60 °C, the presence of H₂O completely inhibits the production of HMF, compared to a yield of 55% when no water was present, in a pure DMSO system. In the presence of the HSO₃-MSN catalyst, we were able to generate HMF and maintain a yield of over 60% when the water content was less than 33 vol%. However, the HMF yield decreased to less than 20% when the water content exceeded 50 vol%, indicating that an increase in water content causes a decrease of the HMF yield. This is because the fructose-to-HMF conversion is a dehydration reaction, and the presence of water disturbs the equilibrium required for the formation of HMF. We obtained similar results for a different organic solvent (i.e., THF) system. Therefore, we determined that the optimal water content was 10 vol% [i.e., an aqueous/DMSO (v/v) ratio of 1:10; see Supporting Information, Table S2].

The third factor affecting HMF yield is the amount of the catalyst. Figure 1(c) indicates that for the same reaction conditions (15 mg of fructose, 10% water content, and a temperature of 60 °C), the yield of HMF increased as the amount of HSO₃-MSN catalyst increased (from 2 to 150 mg). The HMF yield peaked at 150 mg and retained the same value even when more than 150 mg of catalyst was present. Therefore, we determined that 150 mg was the optimal amount of catalyst (Supporting Information, Table S3).

Comparing the effects of the various acidic groups of the MSN catalysts on the fructose-to-HMF conversion provided valuable information. We synthesized three organic-acid-function-

alized MSNs (i.e., COOH-MSN, H₂PO₃-MSN, and HSO₃-MSN) for the production of HMF under the same reaction conditions. Figure 1(d) illustrates that HSO₃-MSN was far more effective than the other two MSNs for both fructose conversion and HMF yield. Acid density and strength of these three acid-functionalized MSNs were measured by IR and ²⁹Si NMR spectroscopic characterization (data not shown), and the results showed that strong Brønsted acid sites in HSO₃-MSN with a high amount of 1.29 mmol(H⁺)g⁻¹ were more effective for the fructose-to-HMF conversion as compared to the as-synthesized MSN sample. Several previous studies have provided similar results by using mesoporous materials and specially designed ionic liquids.^[1b,9]

To demonstrate the successful integration of the enzymatic (water) reaction with the chemical (DMSO) reaction, we attempted to perform a glucose-to-fructose and fructose-to-HMF cascade conversion. Conditions for the glucose-to-fructose reaction were as follows: phosphate buffer, pH 7.5, reaction temperature = 70 °C, reaction time = 24 h, catalyst = isomerase-Fe₃O₄@MSN (15 mg). After the reaction, we separated the isomerase-Fe₃O₄@MSN catalyst by using a magnet, and then added the DMSO and HSO₃-MSN catalyst. Conditions for the fructose-to-HMF reaction were as follows: phosphate buffer/DMSO mixed solution (water content = 10 vol%), reaction time = 15 h, amount of catalyst = 150 mg. Entries 1 to 3 in Table 2 indicate that the reaction temperature has a substantial influence on the final yield of HMF. At room temperature, the HMF yield was nearly zero and the amount of fructose was the

Table 2. Production of HMF from glucose through a glucose-to-fructose-to-HMF sequential reaction.^[a]

Entry	T [°C]	Conversion [%]	Fructose [mg]	Yield of HMF [%]
1	27	57.8	0.045	0
2	60	66.3	0.005	46.1
3	90	70.5	0	45.6
4 ^[b]	60	63.8	0.009	40.1
5 ^[c]	60	56.3	0	4.1
6 ^[d]	60	55.1	0	3.7

[a] Reaction conditions for cellulose-to-glucose: phosphate buffer, pH 4.8, T = 50 °C, t = 24 h, catalyst = cellulase-Fe₃O₄@MSN (15 mg). Reaction conditions for glucose-to-fructose: phosphate buffer, pH 7.5, T = 70 °C, t = 24 h, catalyst = isomerase-Fe₃O₄@MSN (15 mg). Reaction conditions for fructose-to-HMF: phosphate buffer/DMSO mixed solution (water content = 10 vol.%), t = 15 h, catalyst = HSO₃-MSN (0.15 g). [b] Catalyst = HSO₃-MSN (0.1 g). [c] No isomerase-Fe₃O₄@MSN. [d] No phosphate buffer.

highest, indicating that the cascade reaction stopped after fructose conversion. This result is consistent with the aforementioned optimization of the fructose-to-HMF reaction. Although an increased temperature (i.e., 90 °C) increases glucose conversion, the final HMF yield did not increase as it did when the temperature was 60 °C. The results of entries 2 and 4 suggest that the amount of catalyst affects the conversion of fructose and the final yield of HMF. As negative controls, when the isomerase-Fe₃O₄@MSN catalyst was not added in the phosphate buffer (entry 6) or was absent from the glucose-to-fructose reaction (entry 5), the subsequent fructose-to-HMF reaction did not succeed, even with the addition of the HSO₃-MSN catalyst. These results indicate that the source of the second step of the fructose-to-HMF conversion (i.e., fructose) is the product of the first step of the glucose-to-fructose conversion.

Finally, we used cellulose as starting material and demonstrated the cellulose-to-glucose-to-fructose-to-HMF cascade reaction. We previously optimized the reaction conditions for the sequential cellulose-to-glucose and glucose-to-fructose conversions by using cellulase-Fe₃O₄@MSN and isomerase-Fe₃O₄@MSN as the respective catalysts (Supporting Information, Table S4). To cascade two enzymes, we used the same medium (i.e., phosphate buffer) for cellulase and isomerase.^[7d] Therefore, after the cellulose-to-glucose conversion, we simply collected the cellulase-Fe₃O₄@MSN catalyst by using a magnet, increased the reaction temperature to 70 °C and the pH value to 7.4, and added the second catalyst isomerase-Fe₃O₄@MSN. After the glucose-to-fructose conversion, we again collected the isomerase-Fe₃O₄@MSN catalyst by using a magnet, decreased the reaction temperature to 60 °C, and added the third catalyst (HSO₃-MSN) and the organic solvent (DMSO) (maintaining the 1:10 ratio of buffer to DMSO). After reacting for 15 h, the final yield of HMF reached 45.6%, nearly the same as that using glucose as starting reactant (i.e., 46.1%). In this reaction, the strongly acidic property of HSO₃-MSN was useful, unlike weak-acid surface sites of porous materials that act as suitable candidates for biopolymer chain-breaking.^[10,11] The very purpose of utilizing the ionic liquid [BMIM]Cl for the pre-treatment of cellulose is to disrupt the interactions between hydrogen-bonded sheets in cellulose and solvation of microfibrils consisting of a large number of glucan chains, which is possible via disruption mechanism by [BMIM]Cl.^[12(a)] In this case, nucleophilic imidazole can attack and disrupt the hydrogen bonds in cellulose by converting to a mixture of modified cellulose and amorphous cellulose among which later is more prone to enzymatic hydrolysis.^[12(b)]

We then performed the recycle test for the cellulose-to-HMF cascade conversion. Figure 2 indicates that the yield of HMF was similar for each recycle, indicating that the three catalysts used in this study can be successfully recycled while maintaining their catalytic ability. A decrease of HMF yield of ca. 7% from the first to fifth run catalyzed by HSO₃-MSN was found, however, this loss is possibly due to surface deactivation of MSNs and inaccessible HSO₃ groups with each cycles.

Researchers have developed numerous chemocatalytic systems for deconstructing cellulose and performing further conversions,^[13] however, few cellulose deconstruction strategies

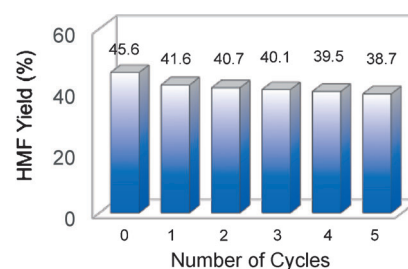


Figure 2. Recyclability test of the HSO₃-MSN for the HMF production in an integrated, cascading method of cellulose conversion.

(e.g., ionic liquid, aqueous media, mechanochemical)^[14] offer selective production of HMF. Compared to these techniques, we integrated enzymatic and chemocatalytic processes, and the whole sequence can be triggered by selecting the desired catalysts, controlling the pH value of the phosphate, and switching the reaction medium from aqueous (enzymatic) to organic (chemocatalytic) at the appropriate steps. These unique features ultimately provide a higher yield of HMF than do the aforementioned strategies.

In summary, we report for the first time an integrated enzyme cascade with a chemocatalytic step for cellulose-to-HMF conversion. This study demonstrates how cellulose deconstruction can be achieved using an enzyme cascade reaction, using Fe₃O₄-loaded, enzyme-immobilized mesoporous silica nanoparticles (MSN) materials that can be easily separated from the reaction medium at each step by applying an external magnetic force. We also demonstrate the effectiveness of the cellulase-immobilized Fe₃O₄@MSN for deconstructing glycosidic bonds of cellulose at pH 4.8, and of isomerase-immobilized Fe₃O₄@MSN for the isomerization of glucose to fructose at pH 7.5, during the cascade reaction sequence. We then integrated enzymatic reactions with the chemocatalytic reaction of the fructose-to-HMF conversion by optimizing several critical factors, such as reaction temperature, ratio of water to organic solvent, and the amount of the acidic catalyst HSO₃-MSN, which caused the entire process to be a one-vessel cascade reaction, offering cellulose deconstruction under milder enzymatic conditions, and generating a high HMF yield of 45%. The results obtained in this study indicate that the concept of integrating enzymatic and chemocatalytic biomass processing can be an effective and economically friendly process for various catalytic applications.

Experimental Section

Chemicals: Poly(oxyethylene) oleyl ether (Brij-97, C₁₈H₃₅EO₁₀), ammonia hydroxide (37%), hydrochloride acid (37%), iron(II) chloride tetrahydrate, 3-aminopropyltrimethoxysilane (APTMS, 97%), dimethyl phthalate (DOP), tetraethoxysilane (TEOS), ethanol (99.8%), cellulase (*Trichoderma reesei* ATCC 26921), 1-butyl-3-methyl-imidazolium chloride (BMIM), cellulose (powder, ca. 20 μm), D-(+)-glucose (>99.5%), D-(-)-fructose (>99%), sodium phosphate tribasic, magnesium sulphate, and sodium chloride were purchased from Sigma-Aldrich (Taipei, Taiwan). Citric acid, sodium hydroxide (NaOH), and acetonitrile were purchased from J. T. Baker. Iron(III) chloride hexahydrate (FeCl₃·6H₂O) was purchased from Alfa Aesar.

Methyl alcohol was purchased from Mallinckrodt Chemical. Glucose isomerase (purified from *Streptomyces rubiginosus*) was purchased from Hampton Research. Organosilanes, such as 3-mercaptopropyltrimethoxysilane (MPTMS), 2-carbomethoxyethyltrimethoxysilane (CTES), and diethylphosphatoethyltriethoxysilane (DPTS), were purchased from Gelest.

Synthesis of magnetite (Fe₃O₄) nanoparticles: FeCl₃ (hexahydrate, 1.349 g) and FeCl₂ (tetrahydrate, 0.781 g) were dissolved into deionized water (600 mL) by stirring, followed by the addition of ammonia hydroxide (1.5 M) to the iron-containing aqueous solution until the pH value of the medium increased to 9. The iron oxide (i.e., Fe₃O₄) product was collected using external magnetic force and washed several times by using deionized water and ethanol. The resulting sample was re-dispersed in 600 mL of deionized water for further use.

Synthesis of Fe₃O₄-loaded MSN: Fe₃O₄-loaded MSN was synthesized using a co-condensation method as follows. Brij-97 (6.92 mL) was added to 180 mL (removed from 600 mL) of magnetite-containing aqueous solution with stirring at room temperature. After a complete dissolution of Brij-97, APTMS (0.3 mL) and DOP (0.8 mL) were added to the Brij-97-magnetite-contained medium with stirring. After stirring for 30 min, TEOS (6.7 mL) was introduced to the magnetite/Brij-97/APTMS/DOP solution, and the mixture was stirred at RT for 1 d, followed by refluxing at 100 °C for another 24 h. Finally, the precipitate was collected through filtration, washed several times by using methanol to remove the surfactant, and dried in lyophilizer. The resulting sample is denoted as Fe₃O₄@MSNs.

Enzyme immobilization: For immobilization of cellulase, Fe₃O₄@MSN (50 mg) was suspended in a citric buffer (10 mM, 2 mL, pH 4.8). To this suspension, 1 mL of cellulase solution was added, and the whole mixture was stirred at 4 °C for 1 d. For immobilization of isomerase, the same amount of Fe₃O₄@MSN was suspended in a phosphate buffer (20 mM sodium phosphate/0.15 M sodium chloride/5 mM magnesium sulfate, pH 7.5). Isomerase solution (0.5 mL) was then added to the phosphate buffer and the whole mixture was stirred at 4 °C for 1 d. Finally, the enzyme-immobilized, Fe₃O₄-loaded MSNs (denoted as cellulase-Fe₃O₄@MSN and isomerase-Fe₃O₄@MSN) were collected using a magnet. The enzyme remaining in the supernatant was considered as a non-adsorbed enzyme, and the amount was measured using a UV-Vis spectrometer at a wavelength of 280 nm. The final catalysts were washed several times by using either a citric (for cellulase) or a phosphate (for isomerase) buffer, and re-dispersed into a citric or a phosphate buffer for further use.

Functionalization of MSN with varying acid functional groups: 1 g of MSN was placed into a two-neck round-bottom flask, and then degassed in vacuum at 110 °C for 30 min. Toluene (30 mL) was then added to the flask in nitrogen atmosphere. For functionalization of the sulfonic group (SO₃H), MPTMS (2.23 mL) was added and the whole system was refluxed at 110 °C. After reacting for 1 d, the thiol-functionalized MSN sample was collected through centrifugation. The thiol group (SH) on the MSN was further converted into a sulfonic group (SO₃H) by reacting SH-MSN with H₂O₂ at RT for 1 d. The final SO₃H-functionalized MSN was collected and dried in vacuum. Similarly, for functionalization of the carboxylic group (COOH), CTES (2.66 mL) was first grafted onto MSN in a toluene system at 110 °C for 1 d. The sample (0.6 g) was then further treated with H₂SO₄ (48 wt%, 90 mL) at 95 °C for 1 d. For functionalization of the phosphoric group (H₂PO₃), DPTS (3.88 mL) was grafted onto MSN in a toluene system at 110 °C for 1 d. The sample (0.6 g) was then further treated with HCl (37 wt%, 10 mL) at 90 °C for 1 d.

Pretreatment of cellulose with ionic liquids: Cellulose (50 mg) was introduced into an ionic liquid (i.e., [BMIM]Cl, 0.95 mL) by stirring at 120 °C for 1 h. Methanol (3 mL) was added to the mixture to quench the reaction and the resulting oligomer was separated from the ionic liquid through centrifugation followed by washing several times, by using methanol and water, and drying in lyophilizer.

Characterization of MSN-based catalysts: The morphology of MSN-based catalysts was analyzed by using scanning electron microscopy (Nova Nano SEM) and transmission electron microscopy (JEOL JEM 2100F). The porous properties were analyzed using nitrogen adsorption/desorption isotherms on a Micromeritics ASAP 2000 instrument. The specific surface area and pore size were calculated using the Brunauer–Emmett–Teller and Barrett–Joyner–Halenda methods, respectively.

Sequential conversion of cellulose involving enzymatic and chemical catalysis: To test the catalytic abilities of free enzymes and immobilized enzymes, ILS-pretreated cellulose (15 mg) was added to a citric buffer (1 mL) containing free cellulase or cellulase-immobilized Fe₃O₄@MSNs at 50 °C for 1 d to cause cellulose-to-glucose conversion. For the glucose-to-fructose conversion, glucose (15 mg) was added to a phosphate buffer (1 mL) containing free isomerase or isomerase-immobilized Fe₃O₄-loaded MSNs at 70 °C for 1 d. For the fructose-to-HMF conversion, fructose (15 mg) was added to a DMSO (5 mL) containing various acid-functionalized MSNs (15 mg) at 60 °C for 1 d. For the cellulose-to-HMF conversion, a sequential cellulose-to-glucose, glucose-to-fructose, and fructose-to-HMF reaction was catalyzed using three separate MSN-based catalysts (i.e., cellulase-immobilized Fe₃O₄@MSNs for the first step, isomerase-immobilized Fe₃O₄@MSNs for the second step, and SO₃H-functionalized MSNs for the third step). Typically, cellulase-immobilized Fe₃O₄@MSNs (15 mg) were added to a phosphate buffer (pH 4.8, 1 mL) containing ILS-pretreated cellulose (15 mg) at 50 °C. After reacting for 1 d, the cellulase-immobilized Fe₃O₄@MSNs were collected using a magnet, and the supernatant was transferred to another vial that contained isomerase-immobilized Fe₃O₄@MSNs (15 mg). Sodium hydroxide was then added to adjust the pH value of the system to 7.5, and the reaction was conducted for another day at 70 °C. After reaction, isomerase-immobilized Fe₃O₄@MSNs were collected using an external magnet, and the supernatant was transferred to another vial that contained DMSO and HSO₃-functionalized MSNs (15 mg). The reaction was run for 1 d at 60 °C to obtain HMF as a final product.

Analysis of products: The products after reaction were analyzed using a high-performance liquid chromatography system (ASI500 system) equipped with a Shodex NH2P50 4E column. Before the products were subjected to HPLC, impurities were removed using a syringe filter. Possible products such as cellobiose, glucose, fructose, and HMF were identified prior to product analysis, and calibration curves were measured. The definition of conversion and yield is described in the Supporting Information.

Acknowledgements

This research was supported by the Ministry of Science and Technology (MOST) of Taiwan (101-2628-E-002-015-MY3, 101-2623-E-002-005-ET, 101-2923-E-002-012-MY3, and 103-2218-E-002-101) of National Taiwan University (101R7842 and 102R7740), and the Center of Strategic Materials Alliance for Research and Technology (SMART Center) of National Taiwan University (102R104100).

Keywords: biomass · enzyme catalysis · immobilization · mesoporous materials · renewable resources

- [1] a) J. Carlos Serrano-Ruiz, R. Luque, A. Sepulveda-Escribano, *Chem. Soc. Rev.* **2011**, *40*, 5266–5281; b) M. E. Zakrzewska, E. Bogel-Lukasik, R. Bogel-Lukasik, *Chem. Rev.* **2011**, *111*, 397–417; c) P. Gallezot, *Chem. Soc. Rev.* **2012**, *41*, 1538–1558.
- [2] M. E. Himmel, S.-Y. Ding, D. K. Johnson, W. S. Adney, M. R. Nimlos, J. W. Brady, T. D. Foust, *Science* **2007**, *315*, 804–807.
- [3] a) U. T. Bornscheuer, G. W. Huisman, R. J. Kazlauskas, S. Lutz, J. C. Moore, K. Robins, *Nature* **2012**, *485*, 185–194; b) J. A. Rollin, T. K. Tam, Y. H. P. Zhang, *Green Chem.* **2013**, *15*, 1708–1719.
- [4] a) Y. Chi, S. T. Scroggins, J. M. J. Frechet, *J. Am. Chem. Soc.* **2008**, *130*, 6322–6323; b) C. You, H. Chen, S. Myung, N. Sathitsuksanoh, H. Ma, X.-Z. Zhang, J. Li, Y. H. P. Zhang, *Proc. Natl. Acad. Sci. USA* **2013**, *110*, 7182–7187.
- [5] a) A. Katz, M. E. Davis, *Nature* **2000**, *403*, 286–289; b) S. Shylesh, A. Wagoner, A. Seifert, S. Ernst, W. R. Thiel, *Angew. Chem. Int. Ed.* **2010**, *49*, 184–187; *Angew. Chem.* **2010**, *122*, 188–191; c) N. Suzuki, M. B. Zakaria, Y.-D. Chiang, K. C. W. Wu, Y. Yamauchi, *Phys. Chem. Chem. Phys.* **2012**, *14*, 7427–7432.
- [6] a) H. Yamada, C. Urata, Y. Aoyama, S. Osada, Y. Yamauchi, K. Kuroda, *Chem. Mater.* **2012**, *24*, 1462–1471; b) H. Yamada, C. Urata, H. Ujiie, Y. Yamauchi, K. Kuroda, *Nanoscale* **2013**, *5*, 6145–6153; c) M. Nandi, J. Mondal, K. Sarkar, Y. Yamauchi, A. Bhaumik, *Chem. Commun.* **2011**, *47*, 6677–6679; d) K. C.-W. Wu, Y. Yamauchi, *J. Mater. Chem.* **2012**, *22*, 1251–1256; e) Y. Yamauchi, *J. Ceram. Soc. Jpn.* **2013**, *121*, 831–840.
- [7] a) A. Takimoto, T. Shiomi, K. Ino, T. Tsunoda, A. Kawai, F. Mizukami, K. Sakaguchi, *Microporous Mesoporous Mater.* **2008**, *116*, 601–606; b) S. B. Hartono, S. Z. Qiao, J. Liu, K. Jack, B. P. Ladewig, Z. Hao, G. Q. M. Lu, *J. Phys. Chem. C* **2010**, *114*, 8353–8362; c) R. H.-Y. Chang, J. Jang, K. C.-W. Wu, *Green Chem.* **2011**, *13*, 2844–2850; d) Y.-C. Lee, C.-T. Chen, Y.-T. Chiu, K. C.-W. Wu, *ChemCatChem* **2013**, *5*, 2153–2157.
- [8] a) Y. Roman-Leshkov, J. N. Chheda, J. A. Dumesic, *Science* **2006**, *312*, 1933–1937; b) H. Zhao, J. E. Holladay, H. Brown, Z. C. Zhang, *Science* **2007**, *316*, 1597–1600; c) J. Carlos Serrano-Ruiz, J. A. Dumesic, *Energy Environ. Sci.* **2011**, *4*, 83–99; d) A. S. Amarasekara, L. D. Williams, C. C. Ebede, *Carbohydr. Res.* **2008**, *343*, 3021–3024; e) Y. Y. Lee, K. C.-W. Wu, *Phys. Chem. Chem. Phys.* **2012**, *14*, 13914–13917.
- [9] a) J. B. Binder, R. T. Raines, *J. Am. Chem. Soc.* **2009**, *131*, 1979–1985; b) Z. Huang, W. Pan, H. Zhou, F. Qin, H. Xu, W. Shen, *ChemSusChem* **2013**, *6*, 1063–1069; c) W.-H. Peng, Y.-Y. Lee, C. Wu, K. C.-W. Wu, *J. Mater. Chem.* **2012**, *22*, 23181–23185.
- [10] a) A. Dutta, D. Gupta, A. K. Patra, B. Saha, A. Bhaumik, *ChemSusChem* **2014**, *7*, 925–933; b) M. G. Mazzotta, D. Gupta, B. Saha, A. K. Patra, A. Bhaumik, M. M. Abu-Omar, *ChemSusChem* **2014**, DOI: 10.1002/cssc.201402007; c) Z. Fei, R. Scopelliti, G. Leurenczy, S. Katsyuba, N. Yan, P. J. Dyson, *ChemSusChem* **2014**, DOI: 10.1002/cssc.201301368.
- [11] P.-W. Chung, A. Charmot, O. A. Olatunji-Ojo, K. A. Durkin, A. Katz, *ACS Catal.* **2014**, *4*, 302–310.
- [12] a) A. S. Gross, A. T. Bell, J. W. Chu, *J. Phys. Chem. B* **2011**, *115*, 13433; b) K. Okushita, E. Shikayama, J. Kikuchi, *Biomacromolecules* **2012**, *13*, 1323–1330.
- [13] a) A. Wang, T. Zhang, *Acc. Chem. Res.* **2013**, *46*, 1377–1386; b) N. Ji, M. Zheng, A. Wang, T. Zhang, J. G. Chen, *ChemSusChem* **2012**, *5*, 939–944; c) Z. Tai, J. Zhang, A. Wang, J. Pang, M. Zheng, T. Zhang, *ChemSusChem* **2013**, *6*, 652–658.
- [14] a) B. Kim, J. Jeong, D. Lee, S. Kim, H.-J. Yoon, Y.-S. Lee, J. K. Cho, *Green Chem.* **2011**, *13*, 1503–1506; b) M. Tan, L. Zhao, Y. Zhang, *Biomass Bioenergy* **2011**, *35*, 1367–1370; c) S. Zhao, M. Cheng, J. Li, J. Tian, X. Wang, *Chem. Commun.* **2011**, *47*, 2176–2178; d) B. R. Caes, M. J. Palte, R. T. Raines, *Chem. Sci.* **2013**, *4*, 196–199; e) J. Fan, M. De Bruyn, V. L. Budarin, M. J. Grönnow, P. S. Shuttleworth, S. Breeden, D. J. Macquarrie, J. H. Clark, *J. Am. Chem. Soc.* **2013**, *135*, 11728–11731; f) C. Tian, C. Bao, A. Binder, Z. Zhu, B. Hu, Y. Guo, B. Zhao, S. Dai, *Chem. Commun.* **2013**, *49*, 8668–8670.

Received: June 29, 2014

Revised: August 8, 2014

Published online on September 26, 2014